13TH CANADIAN MASONRY SYMPOSIUM
HALIFAX, CANADA
JUNE 4TH – JUNE 7TH 2017

NUMERICAL MODELLING AND PARAMETRIC ANALYSIS OF A HYBRID UNREINFORCED MASONRY-REINFORCED CONCRETE WALL STRUCTURE

Frederickx, Florian[1]; Vandoren, Bram[2] and Degée, Hervé[3]

ABSTRACT

This contribution deals with the numerical modelling of hybrid unreinforced masonry-reinforced concrete wall structures (i.e. RC and URM walls coupled by reinforced concrete beams or slabs). Although the combination of these materials is used as a bracing system in several countries, oversimplified design assumptions are often applied due to a lack of knowledge of the structural behaviour of such systems. Therefore, this paper aims at improving this knowledge. The numerical campaign resorts to a pushover analysis: the focus is put on the lateral bracing resistance under statically applied loads. A finite element model, proposed in a previous study, is further refined to account for larger drift demands. The experimental campaign which has been carried out at École polytechnique fédérale de Lausanne (EPFL) is used to calibrate the model. The FE-model is proved as able to accurately predict the distribution of axial loads, base shear and base moment between the two walls. In a subsequent stage, the numerical model is used to perform a parametric analysis on global geometric parameters. Preliminary results of this campaign are presented. It is a first step towards an optimisation of the performances of such hybrid unreinforced masonry-reinforced concrete wall structures.

KEYWORDS: *hybrid, lateral resistance, reinforced concrete, unreinforced masonry*

INTRODUCTION

The study of hybrid unreinforced masonry-reinforced concrete (URM-RC) wall structures has gained more attention in recent years. Experimental as well as numerical campaigns were carried out in order to gain insight into their behaviour [1]–[5]. These campaigns showed that, if these structures are laterally loaded, a hybrid response can be observed. The damage is distributed over different storeys, unlike the damage concentration in the bottom storey of a pure masonry wall

[1] PhD student, Hasselt University, Construction Engineering Research Group, Hasselt, Belgium, florian.frederickx@uhasselt.be
[2] Assistant Professor, Hasselt University, Construction Engineering Research Group, Hasselt, Belgium, bram.vandoren@uhasselt.be
[3] Associate Professor, Hasselt University, Construction Engineering Research Group, Hasselt, Belgium, herve.degee@uhasselt.be

structure. The present numerical campaign is based on previous work [6], in which a numerical model was proposed and calibrated with respect to the experimental campaign of Paparo and Beyer [3]. Good results were obtained for relatively small drifts. In this paper, further efforts are presented in order to obtain results for larger drift demands.

In the following section, the initial finite element model will be described. The aforementioned experimental campaign of Paparo and Beyer [3] is used to calibrate the model. Subsequently, the performance of the model is checked, i.e. the model was tested with different external vertical loads and it was pushed towards the right as well as to the left. The final properties of the model will be fixed in this stage. In the last section, the initial results of the parametric analysis are discussed.

TOWARDS A CALIBRATED NUMERICAL MODEL

The reference model (see Figure 1) will be subjected to a static pushover test, even though a quasi-static cyclic pushover test was performed during the experimental campaign of Paparo and Beyer [3]. Since the URM wall degrades if the specimen is pushed towards the right, it was decided to calibrate the model in this loading direction. Consequently, the axial load in the URM wall decreases during the analysis. The external axial loads correspond to TU1 (see Paparo and Beyer [3]), i.e. 400 kN on top of the URM walls and 125 kN on top of the RC walls. The dimensions of the specimen are presented in Figure 1. The thickness of the walls is 0.15 m and the thickness of the beams is 0.45 m.

Modelling strategy

DIANA 9.6 is used to model the specimen. A simplified micro-modelling strategy [7] is adopted in order to model URM. The bricks and RC elements are modelled with 2D plane stress elements, whereas embedded 1D truss elements are used to model the reinforcement [8], for which perfect bond is assumed. The bricks are connected with zero thickness line interface elements (four nodes), which are used to model the head joints as well as the bed joints. A stiff foundation is modelled in order to support the masonry wall. The foundation is restrained in the horizontal and vertical direction. The RC wall is also restrained at its base in both directions (see Figure 1).

Loading

The vertical loads are distributed on top of the upper RC beam, i.e. 400 kN and 125 kN on top of the URM and RC walls, respectively. These values are adjusted in such a way that the reactions match the experimental reaction values at the beginning of the test. These (increased) values take into account the self-weight of the specimen and the weight of the test set-up. In this way, the self-weight is modelled implicitly.

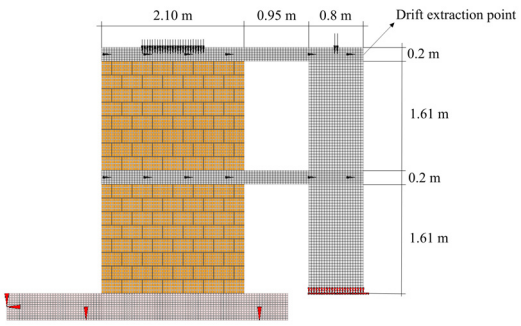

Figure 1: Test set-up

The horizontal load is - proportional to the length of the walls - distributed over the RC beams. This results in an application of the lateral load of approximately 70% at the URM side and 30% at the RC side. In this way, the experimental loading (see Paparo and Beyer [3]) is mimicked. The same lateral load is applied to each beam. Therefore, the analysis is force controlled. In order to capture the complete behaviour, an arc-length method is used.

Material models

All the parameters of the different material models are presented in Table 1 and Table 2. A rotating smeared crack model is used to model the bricks as well as the RC elements. On the sides of the RC walls, the compressive strength was increased in order to take into account the confinement. For the bricks, the mode I fracture energy (G_f^I) and the compressive fracture energy (G_{fc}) were estimated in line with the recommendations of Lourenço [9]. The mode I fracture energy of RC was calculated using Model Code 2010 [10]. However, as presented in a previous study by the authors [6], it was necessary to decrease this value in order to obtain realistic results. The bed joints are modelled with a combined cracking-shearing-crushing material model. The values presented in Table 1 are based on the parameters of Paparo and Beyer [5]. The compressive fracture energy per unit area of the joints was estimated to be approximately 17 Nmm/mm² (Model Code 90). Nevertheless, the degradation of URM due to compressive failure is not captured correctly if this value is assigned. A couple of trial runs showed that 10 N/mm is a better estimation in order to capture the global behaviour. For the head joints, an interface with a discrete crack model was used. Since the head joints are empty, their shear stiffness (K_{tt}) is assumed to be zero and the interfaces' normal stiffness (K_{nn}) is reduced to zero if a very small tensile stress is introduced. The material model of the reinforcement is a von Mises plasticity model with a yield strength f_y = 540 MPa.

Table 1: Material properties bed joints

K_{nn} (N/mm³)	300	f_c (MPa)	5.8	G_f^I (N/mm)	0.41	G_{fc} (N/mm)	10	Ψ (°)	0
K_{tt} (N/mm³)	10	f_t (MPa)	0.3	G_f^{II} (N/mm)	0.5	tan(ϕ)	0.63	c (MPa)	0.38

Table 2: Material properties smeared crack model

Property	Bricks	RC	Property	Bricks	RC
Young's modulus (MPa)	5600	33,000	Mode I fracture energy (N/mm)	0.0406	0.0147
Poisson's coefficient (-)	0.2	0.2	Compressive strength (MPa)	23.5	50 / 80*
Tensile strength (MPa)	1.4	3	Compressive fracture energy (N/mm)	23.12	MC 2010 [10]

* confined concrete

Elastic corner

The model, as presented above, is able to predict a correct behaviour up to approximately 0.3% drift. At this drift demand, numerical problems arise. Initially, it was expected that the damaged interfaces resulted in loose bricks and hence an unstable model. However, different trials showed that this was not the case. The problem was caused by an unexpected local failure at the compressed toe of the bottom RC wall. The application of confined zones in the concrete walls did not prevent the latter issue. In order to overcome this matter, a small elastic corner was implemented. Analyses showed that the presence of this corner did not influence the global behaviour (i.e. the distribution of the axial loads, base shear and base moment, and the load-displacement diagram). The results of the model with the corner and without the corner are almost identical up to the point where damage in the compressed corner occurs.

Results (TU1 - loading towards the right)

The results of the model with an elastic corner and confined zones in the RC walls are depicted in Figure 2 (a-d). These are in close agreement with the experimental results of Paparo and Beyer [3]. The discrepancy in base moment of the URM wall is mainly caused by the differences in axial loads. The numerical load-displacement curve is almost an envelope around the experimental results (Figure 2 d). This indicates that the behaviour is captured well. Figure 3 compares the experimental damage with the predicted numerical damage (the cracked zones are highlighted in Figure 3) at a drift demand of approximately 0.6%. It is clear that the shear cracks, which run through the bricks, are captured at both storeys. Note that the experimental cracks, which are highlighted in Figure 3, are the ones which occurred first in this loading direction. Also the compressive failure of the compressed toe is captured.

Application of self-weight

Up to this point, the self-weight was modelled implicitly, i.e. the axial loads were adjusted in such a way that the experimental reactions were matched. The explicit modelling of the self-weight is necessary in order to perform the intended parametric analysis. The mass of the different elements (URM, RC, loading beams,...) was estimated and initially applied as body loads. Nevertheless, in order to avoid numerical complications, it was decided to distribute the self-weight over the different global elements (walls and beams). The self-weight of the walls is applied at the top and the bottom of the walls (distributed over the length). The load of the beams is also distributed over the length of the beams.

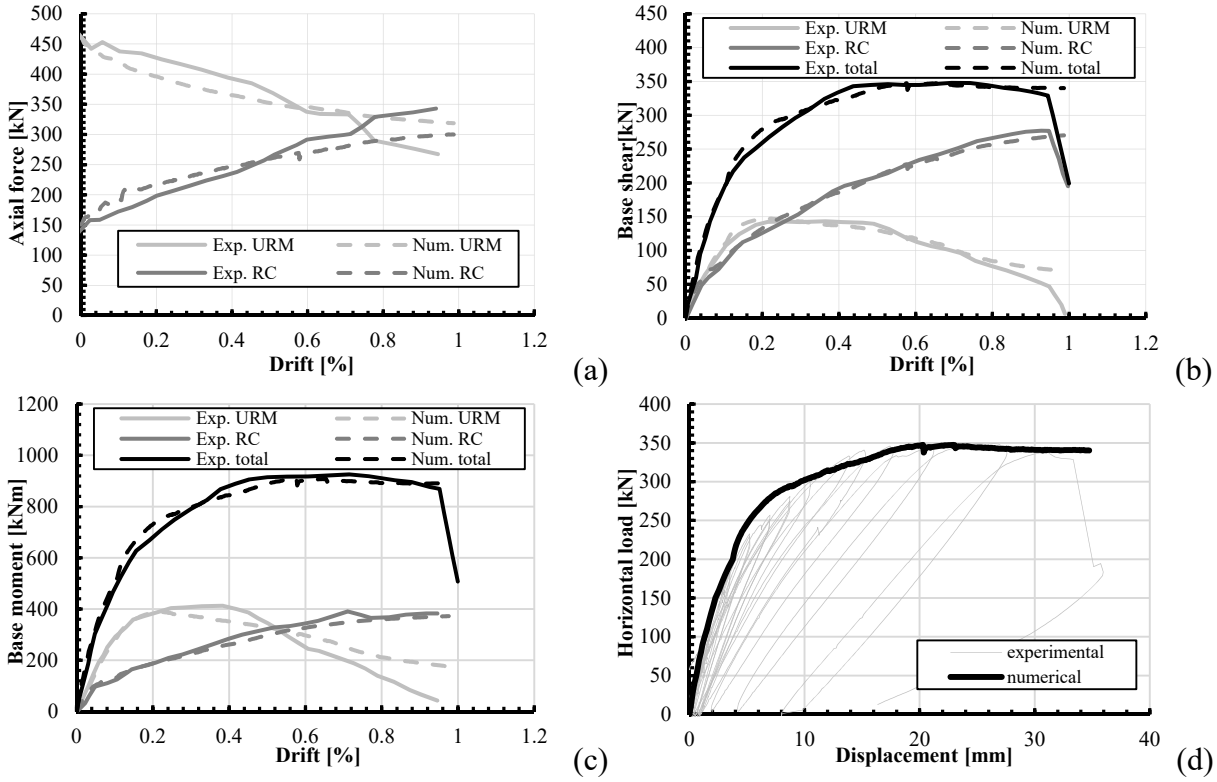

Figure 2: Results TU1, pushing towards RC wall

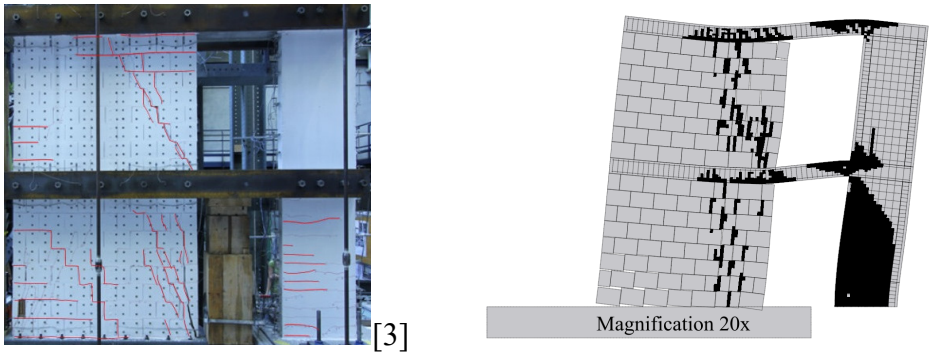

[3]

Figure 3: Experimental damage versus numerical damage (+/- 346 kN)

Performance check

The performance of the calibrated model (TU1, loading towards the right) was evaluated. The model is tested in the other loading direction and it is also tested with a reduced external vertical load (TU2, see Paparo and Beyer [3]) in both loading directions. Some discrepancies were observed and it was therefore necessary to adjust different parameters (compressive fracture energy of the bed joints; compressive strength of masonry and the mode I fracture energy of concrete) in order to match the experimental and numerical results for these different cases.

A final set of material properties is required to perform the parametric analysis. It was therefore decided to change only the compressive fracture energy of the bed joints and the compressive

strength of masonry. The original values, as presented in Table 1, are replaced by 16 N/mm and 6.5 MPa, respectively. This 'best average' approach will result in discrepancies, since the compressive fracture energy controls the compressive failure of masonry. This is necessary to capture the softening of the URM walls (loading towards the right).

RESULTS OF THE CALIBRATED MODEL

The final results, with the fixed parameters for all load cases, are presented in Figure 4 and Figure 5. Due to these fixed parameters, some discrepancies can be observed.

The damage of the different models was evaluated. In case of loading towards the left, the damage was not distributed over the two storeys, but concentrated in the bottom URM wall. Compressive failure was observed at the compressed toe of the URM wall. In the experimental campaign, the damage was also more severe at the bottom URM storey. However, some thin shear cracks appeared at the first storey. TU1 loaded towards the right, has the expected damage pattern (see Figure 3). In case of TU2 (loaded towards the right), the numerical model predicts almost no shear cracks which run through the bricks at the bottom storey. However, shear cracks which run partly through the bricks are predicted at the first storey. In the experimental campaign, diagonal cracks which run through the bricks were observed at the bottom storey and a stepped crack was observed at the first storey.

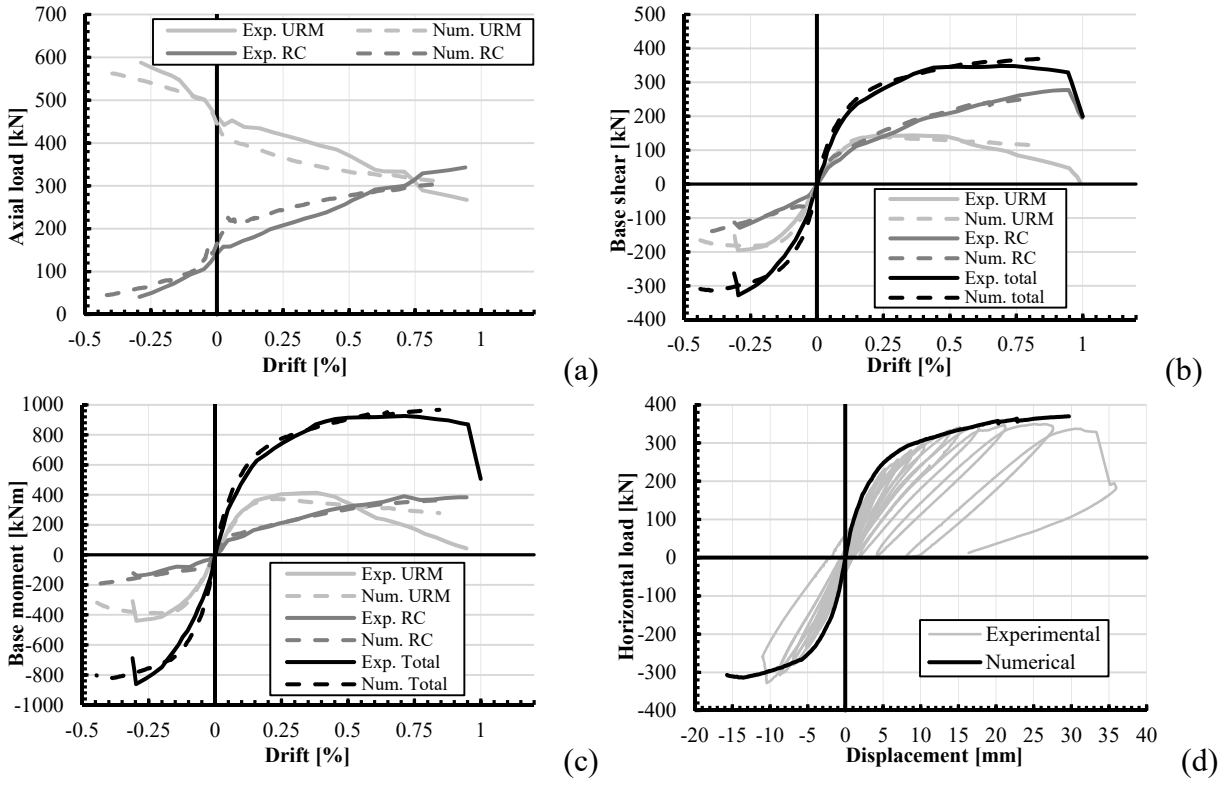

Figure 4: Comparison experimental and numerical results (TU1)

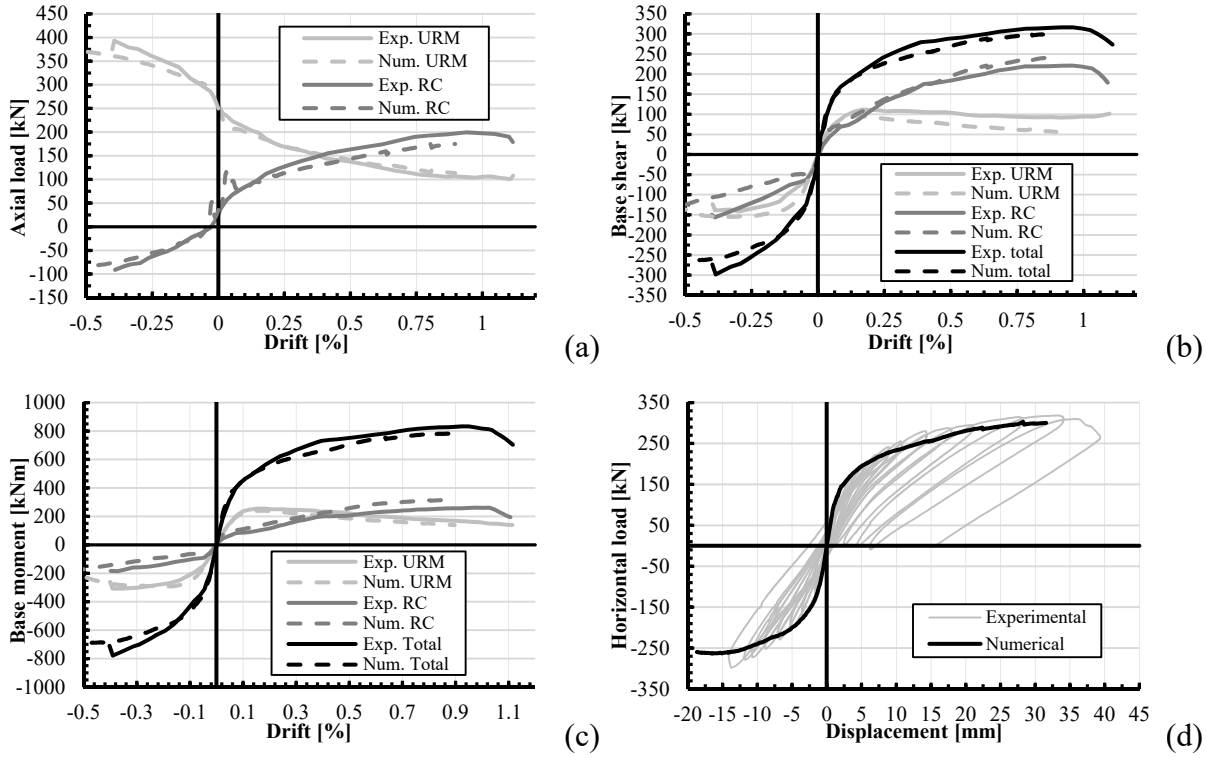

Figure 5: Comparison experimental and numerical results (TU2)

PARAMETRIC ANALYSIS

The calibrated model, in which the self-weight is explicitly modelled, is used to perform a parametric analysis on geometric parameters. As a first step towards optimising this structure, a rough analysis will be performed in order to check the influence of the different parameters, which are presented in Table 3. Case 11 is geometrically the same as the reference structure, but the vertical reinforcement bars in the RC wall have a greater cross section.

Loading

Concerning the self-weight, the following values are assumed: 9.07 kN/m³ and 25 kN/m³ for URM and RC, respectively. The external loads are calibrated in such a way that the initial vertical reaction forces are the same for all cases. There are two load cases and two loading directions. For load case 1, the reaction forces are 440 kN (URM) and 150 kN (RC). These loads are decreased for load case 2, i.e. 240 kN and 35 kN respectively. The horizontal load is entirely applied at the beams' ends. At each storey, an equal lateral load is applied.

Table 3: Parameters parametric analysis

	Ref.	Case 1	Case 2	Case 3	Case 4	Case 5	Case 6	Case 7	Case 8	Case 9	Case 10
Length URM [m]	2.1	3	1.05	2.1	2.1	2.1	2.1	2.1	2.1	2.1	2.1
Length RC [m]	0.8	0.8	0.8	1.2	0.64	0.8	0.8	0.8	0.8	0.8	0.8
Storey height [m]	1.61	1.61	1.61	1.61	1.61	2.41	1.21	1.61	1.61	1.61	1.61
Storeys	2	2	2	2	2	2	2	3	1	2	2
Opening length [m]	0.95	0.95	0.95	0.95	0.95	0.95	0.95	0.95	0.95	1.25	0.65

Results

In this paragraph, the impact of the different global parameters on the distribution of axial loads, base shear and base moment with respect to the drift will be discussed. All the results are plotted against the drift and the values of base shear and base moment are set equal to zero after the application of axial loads (before pushover). In general, the trends are rather similar for load case 1 and load case 2 (with some exceptions). The following results apply to load case 1. A comparison between load case 1 and load case 2 is outside the scope of this paper. The results are presented in Figures 6-8. Concerning Figure 7 and 8, the x-axis is the same for all the curves, but the y-axes differ for each quadrant (i.e. although some graphs are plotted below the y=0 line, the values can be positive and vice versa).

The evolution of the axial loads (with respect to the drift) in the URM wall are depicted in Figure 6. The adjustment of the number of storeys has the greatest influence on the transfer of axial loads. Adding an extra storey results - as expected - in a faster axial load transfer (case 7, black solid line). A single storey hybrid wall displays a slower transfer (case 8, black dashed line). The latter analysis was terminated at a rather low drift demand due to the fact that the solution did not converge. Also an increased storey height should significantly increase the transfer rate of the axial loads. However, this is compensated by the reduced lateral stiffness which can be associated with the increased height of the wall. Hence, the transfer rate is only slightly increased in case of an increased height (case 5, green solid line). The opening length - which does not strongly affect the lateral stiffness - also influences the transfer rate of axial loads significantly. An increased opening length results in a slower transfer and a decreased length in a faster transfer (case 9 and 10 in orange, respectively).

In case of loading towards the left, the variation of the length of the walls barely influences the transfer of axial loads. In the other loading direction, a longer URM wall (case 1, solid blue line) results in a slower transfer. On the contrary, a shorter URM wall or a longer RC wall result in a slightly faster axial load transfer (the results are comparable for both cases, see dashed blue line and solid red line). A shorter RC wall has no significant influence (case 4, dashed red line).

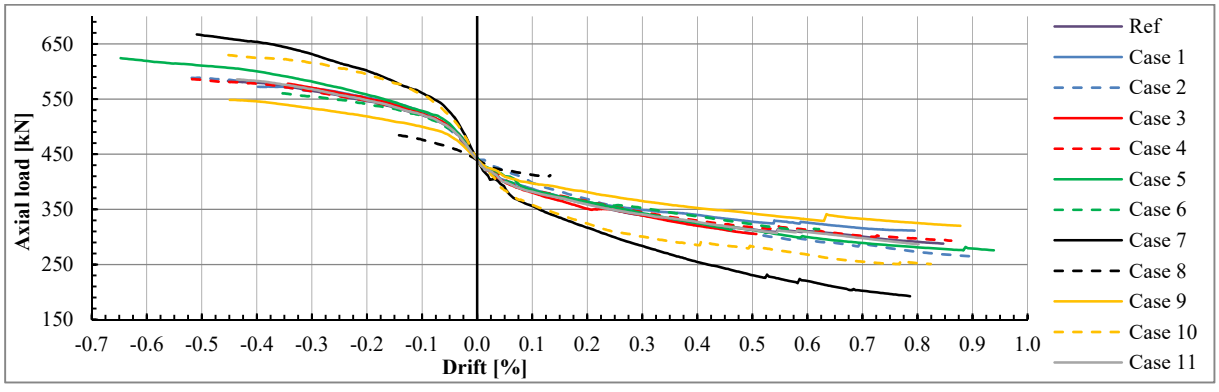

Figure 6: Axial loads URM wall versus drift

The distribution of the base shear, with respect to the drift, is presented in Figure 7. Increasing the length of the URM wall results in an increased base shear in the URM wall as well as in the RC wall (case 1). The opposite is valid for a decreased length (case 2). Nevertheless, the influence on the base shear of the URM wall is much greater in comparison with the base shear of the RC wall (greatest influence of all tested parameters). On the other hand, adjusting the length of the RC wall (case 3 and 4) barely influences the base shear of the URM wall (for load case 2, the influence is greater). The peak base shear (URM) is not influenced, but the lateral load at which it occurs, is affected. The base shear of the RC wall is obviously strongly influenced.

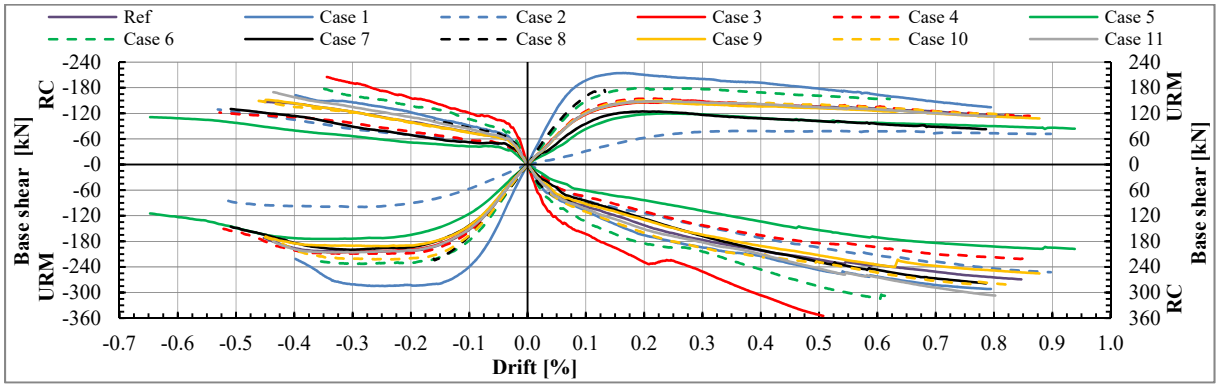

Figure 7: Base shear versus drift

Adjusting the height of the specimen (i.e. number of storeys or storey height) also significantly influences the base shear, e.g. case 5-8 in Figure 7. For the increased values of both cases, the total height is comparable. This results in comparable curves for the base shear of the URM wall if the specimen is loaded towards the right. The peak base shear is decreased in comparison with the reference analysis. The influence on the base shear of the RC wall differs. Increasing the storey height (case 5, solid green line) reduces the base shear in the RC wall significantly and the results in case of adding an extra storey are more comparable to the reference results (within approximately 10%). Adding an extra storey (case 7, solid black line) does not influence the base shear of the URM wall significantly if the specimen is loaded towards the left, but the base shear in the RC wall is reduced. Increasing the storey height results (left loading direction) in a reduced base shear (URM as well as RC). The opposite is valid if the storey height is decreased (case 6, dashed green line). The analysis of a single storey stopped too early due to convergence issues. However, the base shear of the URM wall is increased in both loading directions. It also results in an increased base shear in the RC wall if the specimen is loaded towards the left.

The length of the opening (case 9 and 10, in orange) does not significantly influence the base shear of the URM wall if the specimen is loaded towards the right. The same is applicable to the base shear of the RC wall if the specimen is loaded towards the left. For both situations, an increased opening length results in a lower base shear (compared to the reference results) in the opposite loading direction. A shorter opening results in a greater base shear.

Adjusting the reinforcement bars does not influence the base shear of the URM wall significantly (see Figure 7, case 11 in grey). The base shear of the RC wall is increased, this increase is more noticeable at higher drift demands.

The distribution of base moments is shown in Figure 8. Increasing the length of a certain wall results, as expected, in greater base moments in this wall. Likewise, the base moment of a wall reduces if the length is decreased. Reducing the length of the RC wall (case 4, dashed red line) does not significantly influence the base moment of the URM wall. Increasing the latter length slightly influences the base moment of the URM wall if the specimen is loaded towards the right (10%). In case of an increased URM length (case 1, solid blue line), the base moment of the RC wall is comparable to the reference results. If the URM wall's length is decreased (case 2, dashed blue line), the base moment increases in case of loading towards the right and it decreases if the specimen is pushed towards the left.

Increasing the storey height results in a greater base moment in the URM wall, see case 5 in Figure 8. The RC base moment is reduced (in case of loading towards the right, the base moment is comparable to the one of the reference at higher drift demands). Decreasing the storey height (case 6, dashed green line) leads to reduced URM base moments and slightly greater RC base moments. A single storey structure (case 8) results in lower base moments. Only when the specimen is loaded towards the left, the RC base moment seems to increase. Adding an extra storey (case 7) does not influence the URM base moment significantly if the specimen is loaded towards the right (only valid for load case 1). Nevertheless, the RC base moment is increased. In the other loading direction, the peak URM base moment is increased and the base moments of the RC wall are reduced in comparison with the ones of the reference analysis.

The influence of the length of the opening is rather limited, see case 9 and 10 in Figure 8. Increasing the opening length results in general in slightly greater base moments and a decreased length results in decreased base moments. Except for the base moment of the RC wall in case of loading towards the right, then the opposite is valid.

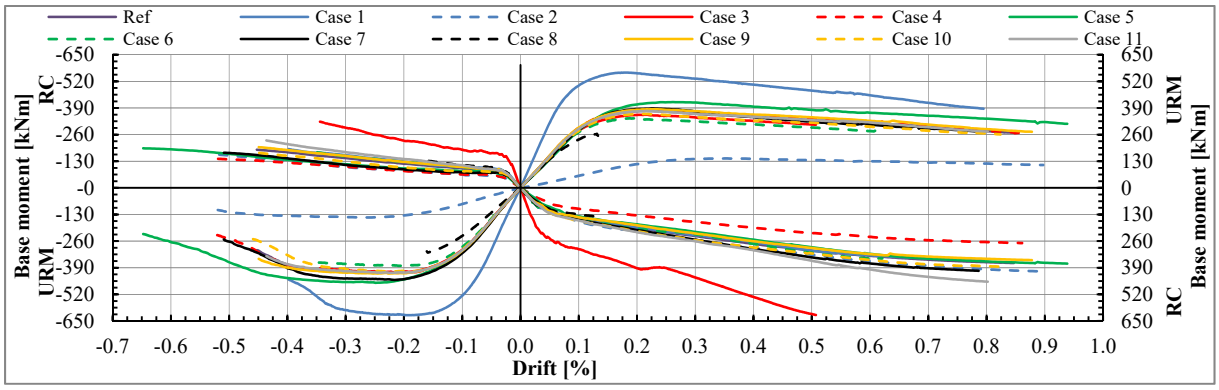

Figure 8: Base moment versus drift

Adjusting the reinforcement bars does not influence the base moment of the URM wall significantly, e.g. case 11 in grey (Figure 8). On the other hand, the base moments of the RC wall are greater than the ones of the reference analysis at similar drift demands.

Finally, the influence on the maximum horizontal load was inspected. Increasing the length of the walls, reducing the height (number of storeys and storey height), decreasing the opening length and increasing the section of the vertical reinforcement bars result in steeper load displacement diagrams and greater maximum lateral loads. The other parameters result in less steep diagrams and lower maximum lateral loads.

CONCLUSION

In this contribution, a fully calibrated finite element model of a hybrid URM-RC wall structure has been presented and improved. The performance of this model was checked (different loading directions and different external axial loads). In order to find good agreement with the experimental results, some parameters demanded various adjustments for different cases. Therefore, averaged parameters were used to perform the parametric analysis. The preliminary results of the presented analysis show the impact of several geometrical properties (length/height of the walls, number of storeys and length of the opening) on the global behaviour of hybrid URM-RC structures.

REFERENCES

[1] K. Beyer, M. Tondelli, S. Petry, and S. Peloso, "Dynamic testing of a four-storey building with reinforced concrete and unreinforced masonry walls: prediction, test results and data set," *Bulletin of Earthquake Engineering*, Apr. 2015.

[2] A. Paparo and K. Beyer, "Seismic behaviour of mixed RC-URM wall structures: comparison between numerical results and experimental evidence," in *Proceedings of the Vienna Congress on Recent Advances in Earthquake Engineering and Structural Dynamics*, 2013.

[3] A. Paparo and K. Beyer, "Quasi-static cyclic tests of two mixed reinforced concrete–unreinforced masonry wall structures," *Engineering Structures*, vol. 71, pp. 201–211, Jul. 2014.

[4] A. Paparo and K. Beyer, "Development of a displacement-based design approach for modern mixed RC-URM wall structures," *Earthquakes and Structures*, vol. 9, no. 4, pp. 789–830, Oct. 2015.

[5] A. Paparo and K. Beyer, "Modelling the seismic response of modern URM buildings retrofitted by adding RC walls," *Journal of Earthquake Engineering*, Nov. 2015.

[6] F. Frederickx, B. Vandoren, and H. Degée, "Finite element modelling of a hybrid unreinforced masonry-reinforced concrete wall," in *Proceedings of the 16th International Brick and Block Masonry Conference*, 2016, pp. 203–210.

[7] P. J. B. B. Lourenço, "Computational strategies for masonry structures," Delft University Press, Delft, Netherlands, 1996.

[8] G.-J. Schreppers, "Embedded Reinforcements." TNO DIANA, Jan-2015.

[9] P. B. Lourenço, "Structural masonry analysis: Recent developments and prospects," 2008.

[10] International Federation for Structural Concrete (FIB), "Model Code for Concrete Structures 2010," 2013.